

Modeling allele-specific gene expression by single-cell RNA sequencing

Yuchao Jiang¹, Nancy R Zhang^{2,*}, Mingyao Li^{3,*}

¹ Genomics and Computational Biology Graduate Program, Perelman School of Medicine, University of Pennsylvania, Philadelphia, PA 19104, USA

² Department of Statistics, The Wharton School, University of Pennsylvania, Philadelphia, PA 19104, USA

³ Department of Biostatistics and Epidemiology, Perelman School of Medicine, University of Pennsylvania, Philadelphia, PA 19104, USA

* To whom correspondence should be addressed. Tel: (+1) 215-746-3916; Fax: (+1) 215-573-1050; Email: nzh@wharton.upenn.edu, mingyao@mail.med.upenn.edu

1 **Abstract**

2 Allele-specific expression is traditionally studied by bulk RNA sequencing, which measures
3 average expression across cells. Single-cell RNA sequencing (scRNA-seq) allows the
4 comparison of expression distribution between the two alleles of a diploid organism and thus the
5 characterization of allele-specific bursting. We propose SCALE to analyze genome-wide allele-
6 specific bursting, with adjustment of technical variability. SCALE detects genes exhibiting allelic
7 differences in bursting parameters, and genes whose alleles burst non-independently. We apply
8 SCALE to mouse blastocyst and human fibroblast cells and find that, globally, *cis* control in
9 gene expression overwhelmingly manifests as differences in burst frequency.

10 **Key words:** single-cell RNA sequencing, expression stochasticity, allele-specific expression,
11 transcriptional bursting, *cis* and *trans* transcriptional control, technical variability.

12 **Background**

13 In diploid organisms, two copies of each autosomal gene are available for transcription, and
14 differences in gene expression level between the two alleles are widespread in tissues [1-7].
15 Allele-specific expression (ASE), in its extreme, is found in genomic imprinting, where the allele
16 from one parent is uniformly silenced across cells, and in random X-chromosome inactivation,
17 where one of the two X-chromosomes in females is randomly silenced. During the last decade,
18 using single-nucleotide polymorphism (SNP)-sensitive microarrays and bulk RNA sequencing
19 (RNA-seq), more subtle expression differences between the two alleles were found, mostly in
20 the form of allelic imbalance of varying magnitudes in mean expression across cells [8-11]. In
21 some cases such expression differences between alleles can lead to phenotypic consequences
22 and result in disease [3, 12-14]. These studies, though revelatory, were at the bulk tissue level,
23 where one could only observe average expression across a possibly heterogeneous mixture of
24 cells.

25 Recent developments in single-cell RNA sequencing (scRNA-seq) have made possible
26 the better characterization of the nature of allelic differences in gene expression across
27 individual cells [6, 15, 16]. For example, recent scRNA-seq studies estimated that 12-24% of the
28 expressed genes are monoallelically expressed during mouse preimplantation development [2]
29 and that 76.4% of the heterozygous loci across all cells express only one allele [17]. These
30 ongoing efforts have improved our understanding of gene regulation and enriched our
31 vocabulary in describing gene expression at the allelic level with single-cell resolution.

32 Despite this rapid progress, much of the potential offered by scRNA-seq data remains
33 untapped. ASE, in the setting of bulk RNA-seq data, is usually quantified by comparing the
34 mean expression level of the two alleles. However, due to the inherent stochasticity of gene
35 expression across cells, the characterization of ASE using scRNA-seq data should look beyond
36 mean expression. A fundamental property of gene expression is transcriptional bursting, in
37 which transcription from DNA to RNA occurs in bursts, depending on whether the gene's
38 promoter is activated (Figure 1A) [18, 19]. Transcriptional bursting is a widespread phenomenon
39 that has been observed across many species including bacteria [20], yeast [21], *Drosophila*
40 embryos [22], and mammalian cells [23, 24], and is one of the primary sources of expression
41 variability in single cells. Figure 1B illustrates the expression across time of the two alleles of a
42 gene. Under the assumption of ergodicity, each cell in a scRNA-seq sample pool is at a different
43 time in this process, implying that for each allele, some cells might be in the transcriptional "ON"
44 state, whereas other cells are in the "OFF" state. While in the "ON" state, the magnitude and
45 length of the burst can also vary across cells, further complicating analysis. For each expressed

46 heterozygous site, a scRNA-seq experiment gives us the bivariate distribution of the expression
47 of its two alleles across cells, allowing us to compare the alleles not only in their mean, but also
48 in their distribution. In this paper, we will use scRNA-seq data to characterize transcriptional
49 bursting in an allele-specific manner and detect genes with allelic differences in the parameters
50 of this process.

51 Kim and Marioni [25] first studied bursting kinetics of stochastic gene expression from
52 scRNA-seq data, using a Beta-Poisson model and estimated the kinetic parameters via a Gibbs
53 sampler. In this early attempt, they assumed shared bursting kinetics between the two alleles
54 and modeled total expression of a gene instead of allele-specific expression. Current scRNA-
55 seq protocols often introduce substantial technical noise (Figure S1) [26-30], and these noise
56 (e.g., gene dropouts, amplification and sequencing bias) are largely ignored in Kim and Marioni
57 [25] and another recent scRNA-seq study Borel et al. [17], where, in particular, gene dropout
58 may have led to overestimation of the pervasiveness of monoallelic expression (ME). Realizing
59 this, Kim et al. [31] incorporated measurements of technical noise from external spike-in
60 molecules into the identification of stochastic ASE (defined as excessive variability in allelic
61 ratios among cells), and concluded that more than 80% of stochastic ASE in mouse embryonic
62 stem cells are due to scRNA-seq technical noise. Kim et al.'s analysis was restricted to the
63 identification of random monoallelic expression (RME) and did not consider more general
64 patterns of ASE such as allele-specific transcriptional bursting.

65 ScRNA-seq also enables us to quantify the degree of dependence between the
66 expressions of the two alleles. A previous RNA fluorescence *in situ* hybridization (FISH)
67 experiment fluorescently labeled 20 genes in an allele-specific manner and showed that there
68 was no significant deviation from independent bursting between the two alleles [32]. A recent
69 scRNA-seq study of mouse cells through embryonic development [2] produced similar
70 conclusions on the genome-wide level: They modeled transcript loss by splitting each cell's
71 lysate into two fractions of equal volume and controlling for false discoveries by diluting bulk
72 RNA down to single-cell level. Their results suggest that on the genome-wide scale, assuming
73 both alleles share the same bursting kinetics, the two alleles of most genes burst independently.
74 Deviation from the theoretical curve in Deng et al. [2] for independent bursting with shared
75 allele-specific kinetics, however, can be due to not only dependent bursting, but also differential
76 bursting kinetics.

77 In this paper, we develop SCALE (**S**ingle-**C**ell **A**llelic **E**xpression), a systematic
78 statistical framework to study ASE in single cells by examining allele-specific transcriptional
79 bursting kinetics. Our main goal is to detect and characterize differences between the two

80 alleles in their expression distribution across cells. As a by-product, we will also quantify the
81 degree of dependence between the expressions of the two alleles. SCALE is comprised of three
82 steps. First, an empirical Bayes method determines, for each *gene*, whether it is silent,
83 monoallelically expressed, or biallelically expressed, based on its allele-specific counts across
84 cells (Figure 1C). Next, for genes determined to be biallelic bursty (i.e., both alleles have zero
85 expression level in some but not all cells), a Poisson-Beta hierarchical model is used to estimate
86 allele-specific transcriptional kinetics while accounting for technical noise and cell size
87 differences. Finally, resampling-based testing procedures are developed to detect allelic
88 differences in transcriptional burst size or burst frequency, and identify genes whose alleles
89 exhibit non-independent transcription.

90 *In silico* simulations are conducted to investigate estimation accuracy and testing power.
91 The stringency of model assumptions, and the robustness of the proposed procedures to the
92 violation of these assumptions, will be discussed as they are introduced. Using SCALE, we re-
93 analyze the scRNA-seq data for 122 mouse blastocyst cells [2] and 104 human fibroblast cells
94 [17]. The mouse blastocyst study initially found abundant RME generated by independent and
95 stochastic allelic transcription [2]; the human fibroblast study reported that 76.4% of the
96 heterozygous loci displayed patterns of ME [17]. Through proper modeling of technical noise,
97 our re-analysis of these two datasets brings forth new insights: While for 90% of the bursty
98 genes, there are no significant deviations from the assumption of independent allelic bursting
99 and shared bursting kinetics, the remaining bursty genes show differential burst frequency by a
100 *cis*-effect and/or non-independent bursting with an enrichment in coordinated bursting.
101 Collectively, we present a genome-wide approach to systematically analyze expression
102 variation in an allele-specific manner with single-cell resolution. SCALE is an open-source R
103 package available at <https://github.com/yuchaojiang/SCALE>.

104 **Results**

105 **Methods overview**

106 Figure 2 shows an overview of the analysis pipeline of SCALE. We start with allele-specific read
107 counts of endogenous RNAs across all profiled single cells. An empirical Bayes method is
108 adopted to classify expression of genes into monoallelic, biallelic, and silent states based on
109 ASE data across cells. SCALE then estimates allele-specific transcriptional bursting parameters
110 via a hierarchical Poisson-Beta model, while adjusting for technical variabilities and cell size
111 differences. Statistical testing procedures are then performed to identify genes whose two

112 alleles have different bursting parameters or burst non-independently. We describe each of
113 these steps in turn.

114 **Gene classification by ASE data across cells.** SCALE first determines for each gene whether
115 its expression is silent, paternal/maternal monoallelic, or biallelic. Figure 1C outlines this
116 categorization scheme. Briefly, for each gene, each cell is assigned to one of four categories
117 corresponding to scenarios where both alleles are off (\emptyset), only A allele is expressed (A), only B
118 allele is expressed (B), and both alleles are expressed (AB). An expectation-maximization (EM)
119 algorithm is implemented for parameter estimation. This classification accounts for both
120 sequencing depth variation and sequencing errors. The assignment of the *gene* is then
121 determined based on the posterior assignments of all cells. For example, if all cells are assigned
122 to $\{\emptyset\}$, the gene is silent; if all cells are assigned to either $\{\emptyset\}$ or $\{A\}$, the gene has ME of the A
123 allele; if all cells are assigned to either $\{\emptyset\}$ or $\{B\}$, the gene has ME of the B allele; if both A and
124 B allele are expressed in the cell pool, then the gene is biallelically expressed. Refer to Methods
125 for detailed statistical method and the EM algorithm.

126 Through simulation studies (under section Assessment of estimation accuracy and
127 testing power), we show that bursting parameters can only be stably estimated for *bursty* genes,
128 that is, genes that are silent in a non-zero proportion of cells. Therefore, for biallelic bursty
129 genes, allele-specific transcriptional kinetics are modeled through a Poisson-Beta distribution
130 with adjustment of technical noise. For silent, monoallelically expressed, or constitutively
131 expressed genes, there is no way nor need to estimate bursting kinetics for both alleles.

132 **Allele-specific transcriptional bursting.** When studying ASE in single cells, it is critical to
133 consider transcriptional bursting due to its pervasiveness in various organisms [20-24]. We
134 adopt a Poisson-Beta hierarchical model to quantify allele-specific transcriptional kinetics while
135 accounting for dropout events and amplification and sequencing bias. Here, we start by
136 reviewing the relevant literature with regard to transcriptional bursting at the single-cell level.

137 A two-state model for gene transcription is shown in Figure 1A, where genes switch
138 between the “ON” and “OFF” states with activation and deactivation rates k_{on} and k_{off} . When
139 the gene is at the “ON” state, DNA is transcribed into RNA at rate s while RNA decays at rate d .
140 A Poisson-Beta stochastic model was firstly proposed by Kepler and Elston [33]:

$$141 \quad Y \sim \text{Poisson}(sp),$$
$$142 \quad p \sim \text{Beta}(k_{on}, k_{off}),$$

143 where Y is the number of mRNA molecules and p is the fraction of time that the gene spends in
144 the active state, the latter having mean $k_{on}/(k_{on} + k_{off})$. Under this model, $1/k_{on}$ and $1/k_{off}$
145 are the average waiting times in the inactive and active states, respectively. *Burst size*, defined
146 as the average number of synthesized mRNA per burst episode, is given by s/k_{off} , and *burst*
147 *frequency* is given by k_{on} . Kepler and Elston [33] gave detailed analytic solutions via differential
148 equations. Raj et al. [23] offered empirical support for this model via single-molecule FISH
149 experiment on reporter genes. Since the kinetic parameters are measured in units of time and
150 only the stationary distribution is assumed to be observed (e.g., when cells are killed for
151 sequencing and fixed for FISH experiment), the rate of decay d is set to one [15]. This is
152 equivalent to having three kinetic parameters $\{s, k_{on}, k_{off}\}$, each normalized by the decay rate d .
153 Kim and Marioni [25] applied this Poisson-Beta model to total gene-level transcript counts from
154 scRNA-seq data of mouse embryonic stem cells. While they found that the inferred kinetic
155 parameters are correlated with RNA polymerase II occupancy and histone modification [25],
156 they didn't address the issue of technical noise, especially the dropout events, introduced by
157 scRNA-seq. Failure of accounting for gene dropouts may lead to biased estimation of bursting
158 kinetics.

159 Furthermore, since the transitions between active and inactive states occur separately
160 for the two alleles, when allele-specific expression data are available, it seems more appropriate
161 to model transcriptional bursting in an allele-specific manner. The fact that transcriptional
162 bursting occurs independently for the two alleles has been supported by empirical evidence:
163 Case studies based on imaging methods have suggested that the two alleles of genes are
164 transcribed in an independent fashion [34, 35]; using scRNA-seq data, Deng et al. [2] showed
165 that the two alleles of most genes tend to fire independently with the assumption that both
166 alleles share the same set of kinetic parameters. These findings, although limited in scale or
167 relying on strong assumptions, emphasize the need to study transcriptional bursting in an allele-
168 specific manner.

169 ***Technical noise in scRNA-seq and other complicating factors.*** Figure S1 outlines the major
170 steps of the scRNA-seq protocols and the sources of bias that are introduced during library
171 preparation and sequencing. After the cells are captured and lysed, exogenous spike-ins are
172 added as internal controls, which have fixed and known concentration and can thus be used to
173 convert the number of sequenced transcripts into actual abundances. During the reverse
174 transcription, pre-amplification, and library preparation steps, lowly expressed transcripts might
175 be lost, in which case they will not be detected during sequencing. This leads to the so-called

176 “dropout” events. Since spike-ins undergo the same experimental procedure as endogenous
177 RNAs in a cell, amplification and sequencing bias can be captured and estimated through the
178 spike-in molecules. Here we adopt the statistical model in TASC (Toolkit for Analysis of Single
179 Cell data, unpublished), which explicitly models the technical noise through spike-ins. TASC’s
180 model is based on the key observation that the probability of a gene being a “dropout” depends
181 on its true expression in the cell, with lowly expressed gene more likely to drop out. Specifically,
182 let Q_{cg} and Y_{cg} be, respectively, the observed and true expression level of gene g in cell c . The
183 hierarchical mixture model used to model dropout, amplification and sequencing bias is:

$$\begin{aligned} 184 \quad Q_{cg} &\sim Z_{cg} \text{Poisson}(\alpha_c (Y_{cg})^{\beta_c}), \\ 185 \quad Z_{cg} &\sim \text{Bernoulli}(\pi_{cg}), \\ 186 \quad \pi_{cg} &= \text{expit}(\kappa_c + \tau_c \log(Y_{cg})), \end{aligned}$$

187 where Z_{cg} is a Bernoulli random variable indicating that gene g is detected in cell c , that is, a
188 dropout event has not occurred. The success probability $\pi_{cg} = P(Z_{cg} = 1)$ depends on $\log(Y_{cg})$,
189 the logarithm of the true underlying expression. Cell-specific parameters α_c models the capture
190 and sequencing efficiency; β_c models the amplification bias; κ_c and τ_c characterize whether a
191 transcript is successfully captured in the library. This model will later be used to adjust for
192 technical noise in allele-specific expression.

193 As input to SCALE, we recommend scRNA-seq data from cells of the same type.
194 Unwanted heterogeneity, however, still persists as the cells may differ in size or may be in
195 different phases of the cell cycle. Through a series of single-cell FISH experiments, Padovan-
196 Merhar et al. [36] showed how gene transcription depends on these exogenous factors: burst
197 size is independent of cell cycle but is kept proportional to cell size by a *trans* mechanism; burst
198 frequency is independent of cell size but is reduced approximately by half, through a *cis*
199 mechanism, between G1 and G2 phase to compensate for the doubling of DNA content. Figure
200 S2 gives an illustration on how burst size and burst frequency change with cell size and cell
201 cycle phase. Note that, while the burst frequency from *each* DNA copy is halved when the
202 amount of DNA is doubled, the total burst frequency remains roughly constant through the cell
203 cycle. Thus, SCALE adjusts for variation in cell size through modulation of burst size, and does
204 not adjust for variation in cell cycle phase. Details will be given below.

205 There are multiple ways to measure cell size. Padovan-Merhar et al. [36] proposed using
206 the expression level of *GAPDH* as a cell size marker. When spike-ins are available, we use the
207 ratio of the total number of endogenous RNA reads over the total number of spike-in reads as a
208 measure (Figure S2) of the total RNA volume, which was shown to be a good proxy for cell size

209 [28]. SCALE allows the user to input the cell sizes ϕ_c , if these are available through other
 210 means.

211 **Modeling transcriptional bursting with adjustment of technical and cell-size variation.** We

212 are now ready to formulate the allele-specific bursting model for scRNA-seq data. For genes
 213 that are categorized as biallelic bursty (with proportion of cells expressing each allele between 5%
 214 and 95% from the Bayes framework), SCALE proceeds to estimate the allele-specific bursting
 215 parameters using a hierarchical model:

$$216 \quad Y_{cg}^A \sim \text{Poisson}(\phi_c s_g^A p_{cg}^A) \quad Y_{cg}^B \sim \text{Poisson}(\phi_c s_g^B p_{cg}^B)$$

$$217 \quad p_{cg}^A \sim \text{Beta}(k_{on,g}^A, k_{off,g}^A) \quad p_{cg}^B \sim \text{Beta}(k_{on,g}^B, k_{off,g}^B),$$

218 where Y_{cg}^A and Y_{cg}^B are the true allele-specific expressions for gene g in cell c . The two alleles of
 219 each gene are modeled by separate Poisson-Beta distributions with kinetic parameters that are
 220 gene- and allele-specific. These two Poisson-Beta distributions share the same cell size factor
 221 ϕ_c , which affects burst size. The true allele-specific expressions Y_{cg}^A and Y_{cg}^B are not directly
 222 observable. The observed allele-specific read counts Q_{cg}^A and Q_{cg}^B are confounded with technical
 223 noise, and follow the Poisson mixture model outlined in the previous section:

$$224 \quad Q_{cg}^A \sim Z_{cg}^A \text{Poisson}(\alpha_c (Y_{cg}^A)^{\beta_c}) \quad Q_{cg}^B \sim Z_{cg}^B \text{Poisson}(\alpha_c (Y_{cg}^B)^{\beta_c})$$

$$225 \quad Z_{cg}^A \sim \text{Bernoulli}(\pi_{cg}^A) \quad Z_{cg}^B \sim \text{Bernoulli}(\pi_{cg}^B)$$

$$226 \quad \pi_{cg}^A = \text{expit}(\kappa_c + \tau_c \log(Y_{cg}^A)) \quad \pi_{cg}^B = \text{expit}(\kappa_c + \tau_c \log(Y_{cg}^B)).$$

227 How to generate input to SCALE for both endogenous RNAs and exogenous spike-ins is
 228 included in Methods and Supplementary Methods. For parameter estimation, we developed a
 229 new “histogram-repiling” method to obtain the distribution of Y_{cg} from the observed distribution of
 230 Q_{cg} . The bursting parameters are then derived from the distribution of Y_{cg} by moment estimators.
 231 Standard errors and confidence intervals of the parameters are obtained using nonparametric
 232 bootstrap. The details are shown in Methods.

233 **Hypothesis testing.** For biallelic bursty genes, we use nonparametric Bootstrap to test the null
 234 hypothesis that the burst frequency and burst size of the two alleles are the same ($k_{on}^A = k_{on}^B$,
 235 $s^A/k_{off}^A = s^B/k_{off}^B$) against the alternative hypothesis that either or both parameters differ
 236 between alleles. For each gene, we also perform chi-square test to determine if the transcription
 237 of the two alleles are independent by comparing the observed proportions of cells from the gene
 238 categorization framework against the expected proportions under independence. For genes
 239 where the proportion of cells expressing both alleles is significantly higher than expected, we

240 define their bursting as coordinated; for genes where the proportion of cells expressing only one
241 allele is significantly higher than expected, we define their bursting as repulsed (Figure 2). We
242 adopt false discovery rate (FDR) to adjust for multiple comparisons. Details of the testing
243 procedures are outlined in Methods.

244 **Analysis of scRNA-seq dataset of mouse cells during preimplantation development**

245 We re-analyze the scRNA-seq dataset of mouse blastocyst cells dissociated from *in vivo* F1
246 embryos (CAST/female x C57/male) from Deng et al. [2]. Transcriptomic profiles of each
247 individual cell was generated using the Smart-seq [37] protocol. For 22,958 genes, reads per
248 kilo base per million reads (RPKM) and total number of read counts across all cells are available.
249 Parental allele-specific read counts are also available at heterozygous loci (Figure S3).
250 Principal component analysis (PCA) was performed on cells from oocyte to blastocyst stages of
251 mouse preimplantation development and showed that the first three principal components well
252 separate the early-stage cells from the blastocyst cells (Figure S4). The cluster of early-, mid-,
253 and late-blastocyst cells are combined to gain sufficient sample size. In discussion, we give
254 further insights on the potential effects of cell subtype confounding. Quality control (QC)
255 procedure was adopted to remove outliers in library size, mean and standard deviation of allelic
256 read counts/proportions. We apply SCALE to this dataset of 122 mouse blastocyst cells, with a
257 focus on addressing the issue of technical variability and modeling of transcriptional bursting.

258 Eight exogenous RNAs with known serial dilutions are added in late blastocyst cells
259 (Table S1A) and are used to estimate the technical-noise associated parameters (Figure S5A).
260 We apply the Bayes gene classification framework to these cells to get the genome-wide
261 distribution of gene categories. Specifically, out of the 22,958 genes profiled across all cells,
262 ~43% are biallelically expressed (~33% of the total are biallelic bursty and ~10% of the total are
263 biallelic non-bursty), ~7% are monoallelically expressed, and ~50% are silent. Our empirical
264 Bayes categorization results show that, on the genome-wide scale, the two alleles of most
265 biallelic bursty genes share the same bursting kinetics and burst independently (Figure S6A), as
266 has been reported by Deng et al. [2].

267 For the 7,486 genes that are categorized as biallelic bursty, we apply SCALE to identify
268 genes whose alleles have different bursting kinetic parameters by the Bootstrap-based
269 hypothesis tests as previously described. After FDR control, we identify 425 genes whose two
270 alleles have significant differential burst frequency (Figure 3A) and 2 genes whose two alleles
271 have significant differential burst size (Figure 3B). Figure 4 shows the allelic read counts of a
272 gene that has differential burst frequency (*Btf3l4*) and a gene that has differential burst size

273 (*Fdps*). The two genes with significant differential allelic burst size, namely, gene *Fdps* and
274 *Atp6ap2*, are also significant in having differential burst frequency between the two alleles. *P*-
275 values from differential burst frequency testing have a spike below the significance level after
276 FDR control (Figure 3A), while those from differential burst size testing are roughly uniformly
277 distributed (Figure 3B).

278 At the whole genome level, these results show that allelic differences in the expression
279 of bursty genes during embryo development is achieved through differential modulation of burst
280 frequency rather than burst size. This seems to agree with intuition, since allelic differences
281 must be caused by factors that act in *cis* to regulate gene expression, and *cis* factors are likely
282 to change burst frequency by affecting promoter accessibility [36, 38-40]. On the contrary, while
283 it is plausible for *cis* factors to affect allelic burst size through, for example, the efficiency of RNA
284 Polymerase II recruitment or the speed of elongation, the few known cases of burst size
285 modulation are controlled in *trans* [36]. Furthermore, previous studies have shown that the
286 kinetic parameter that varies the most – along the cell cycle [36], between different genes [41],
287 between different growth conditions [42], or under regulation by a transcription factor [43] – is
288 the probabilistic rate of switching to the active state k_{on} , while the rates of gene inactivation k_{off}
289 and of transcription s vary much less.

290 Our analysis includes 107 male cells ($X^A Y$) and 15 female cells ($X^A X^B$) and this allows us
291 to use those bursty X-chromosome genes as positive controls. As a result of this gender mixture,
292 there are more cells expressing the maternal X^A allele compared to the paternal X^B allele. As
293 shown in Figure 3, SCALE successfully detects these bursty X-chromosome genes with
294 significant difference in allelic burst frequency but not in allelic burst size. If we only keep the
295 107 male cells, these X-chromosome genes are correctly categorized as monoallelically
296 expressed – the bursting kinetics for the paternal X^B allele are not estimable – and in this case
297 there is no longer a cluster of significant X-chromosome genes separated from the autosomal
298 genes (Figure S8).

299 For biallelic bursty genes, we also used a simple Binomial test to determine if the mean
300 allelic coverage across cells is biased towards either allele. This is comparable to existing tests
301 of allelic imbalance in bulk tissue, although the total coverage across cells in this dataset is
302 much higher than standard bulk tissue RNA-seq data. After multiple hypothesis testing
303 correction, we identify 417 genes with significant allelic imbalance, out of which 238 overlap with
304 the significant genes from the testing of differential bursting kinetics (Figure 5A). Inspection of
305 the estimated bursting kinetic parameters in Figure 5A shows that, when the burst size and
306 burst frequency of the two alleles change in the same direction (e.g., gene *Gprc5a* in Figure 5B),

307 testing of allelic imbalance can detect more significant genes with higher power. This is not
308 unexpected – a small insignificant increase in burst size adds on top of an insignificant increase
309 in burst frequency resulting in a significant increase in overall expression levels between the two
310 alleles. However, for genes in red in the top left and bottom right quadrants of Figure 5A, the
311 test for differential bursting kinetics detects more genes than the allelic imbalance test. This is
312 due to the fact that when burst size and burst frequency change in opposite directions (e.g.,
313 gene *Dhrs7* in Figure 5B), their effects cancel out when looking at the mean expression.
314 Furthermore, even when the burst size does not change, if the change in burst frequency is
315 small, by using a more specific model SCALE has higher power to detect it as compared to an
316 analysis based on mean allelic imbalance. Overall, the allelic imbalance test and differential
317 bursting test report overlapping but substantially different set of genes, with each test having its
318 benefits. Compared to the allelic imbalance test, SCALE gives more detailed characterization of
319 the nature of the difference by attributing the change in mean expression to a change in the
320 burst frequency and/or burst size.

321 It is also noticeable that in Figure 5A the vertical axis, $\Delta freq$, has a 50% wider range
322 than the horizontal axis, $\Delta size$. Therefore, while it is visually not obvious from this scatter plot,
323 there are much more genes with large absolute $\Delta freq$ than with large absolute $\Delta size$. Although
324 the standard errors of these estimated differences are not reflected in the plot, given our testing
325 results, those genes with large estimated differences in $\Delta size$ also have large standard errors in
326 their estimates, which is further confirmed via simulations.

327 Further chi-squared test of the null hypothesis of independence (Figure 4C) shows that
328 there are 424 genes whose two alleles fire in a significantly non-independent fashion. We find
329 that all significant genes have higher proportions of cells expressing both alleles than expected,
330 indicating coordinated expression between the two alleles. In this dataset, there are no
331 significant genes with repulsed bursting between the two alleles. Repulsed bursting, in the
332 extreme case where at most one allele is expressed in any cell, is also referred to as stochastic
333 ME [31]. Our testing results indicate that, in mouse embryo development, all cases of stochastic
334 ME (i.e., repulsion between the two alleles) can be explained by independent and infrequent
335 stochastic bursting. The burst synchronization in the 424 significant genes is not unexpected
336 and is possibly due to a shared *trans* factor between the two alleles (e.g., co-activation of both
337 alleles by a shared enhancer). This result is concordant with the findings from a mouse
338 embryonic stem cell scRNA-seq study by Kim et al. [31], which reported that the two alleles of a
339 gene show correlated allelic expression across cells more often than expected by chance,

340 potentially suggesting regulation by extrinsic factors [31]. We further discuss the sharing of such
341 extrinsic factors under the context of cell population admixtures in Discussion.

342 In summary, our results by SCALE suggest that: (i) The two alleles from 10% of the
343 bursty genes show either significant deviations from independent firing or significant differences
344 in bursting kinetic parameters, (ii) For genes whose alleles differ in their bursting kinetic
345 parameters, the difference is found mostly in the burst frequency instead of the burst size, (iii)
346 For genes whose alleles violate independence, their expression tends to be coordinated. Refer
347 to Table S1B for genome-wide output from SCALE.

348 **Analysis of scRNA-seq dataset of human fibroblast cells**

349 To further examine our findings in a dataset without potential confounding of cell type
350 admixtures, we apply SCALE to a scRNA-seq dataset of 104 cells from female human newborn
351 primary fibroblast culture from Borel et al. [17]. The cells were captured by Fluidigm C1 with 22
352 PCR cycles and were sequenced with on average 36 million reads (100 bp, paired end) per cell.
353 Bulk-tissue whole genome sequencing was performed on two different lanes with 26-fold
354 coverage on average and was used to identify heterozygous loci in coding regions. After QC
355 procedures, 9016 heterozygous loci from 9016 genes were identified (if multiple loci coexist in
356 the same gene, we pick the one with the highest mean depth of coverage). At each locus, we
357 use SAMtools [44] mpileup to obtain allelic read counts in each single cell from scRNA-seq,
358 which are further used as input for SCALE. 92 ERCC synthesized RNAs were added in the lysis
359 buffer of 12 fibroblast cells with a final dilution of 1:40000. The true concentrations and the
360 observed number of reads for all spike-ins are used as baselines to estimate technical variability
361 (Table S1C, Figure S5B). Refer to Supplementary Methods for details on the bioinformatic
362 pipeline.

363 We apply the gene categorization framework by SCALE and find that out of the 9016
364 genes, the proportions of monoallelically expressed, biallelically expressed, and silent genes are
365 11.5%, 45.7%, and 42.8%, respectively. For the 2277 genes that are categorized as biallelic
366 bursty, we estimate their allele-specific bursting kinetic parameters and find that the correlations
367 between the estimated burst frequency and burst size between the two alleles are 0.859 and
368 0.692 (Figure 6). We then carry out hypothesis testing on differential allelic bursting kinetics.
369 After FDR correction, we identified 26 genes with significant differential burst frequency between
370 the two alleles (Figure 6A) and one gene *Nfx1* with significantly differential burst size between
371 the two alleles, which is also significant in burst frequency testing (Figure 6B). We further carry
372 out testing of non-independent bursting between the two alleles and identify 35 significant genes

373 after FDR correction (Figure S6B). Out of the 35 significant genes, 27 showed patterns of
374 coordinated bursting while the rest 8 showed repulsed patterns. Refer to Table S1D for detailed
375 output from SCALE across all tested genes.

376 We also carry out pairwise correlation analysis between the estimated allelic bursting
377 kinetics, the proportion of unit time that the gene stays in the active state $k_{on}/(k_{on} + k_{off})$ for
378 each allele, as well as the overall allele-specific expression levels (taken as the sum across all
379 cells at the heterozygous locus). Notably, we find that the overall allele-specific expression
380 correlates strongly with the burst frequency and the proportion of time that the gene stays active,
381 but not with the burst size (Figure S9), in concordance with Kim and Marioni [25]. This further
382 supports our previous conclusion that the allele-specific expression at single-cell level manifests
383 as differences in burst frequency in a *cis*-manner.

384 **Assessment of estimation accuracy and testing power**

385 First, we investigate the accuracy of the moment estimators for the bursting parameters under
386 four different scenarios in the Poisson-Beta transcription model: (i) small k_{on} and small k_{off} ,
387 which we call bursty and leads to relatively few transitions between the “ON” and “OFF” state
388 with a bimodal mRNA distribution across cells (Figure S10A); (ii) large k_{on} and small k_{off} , which
389 leads to long durations in the “ON” state and resembling constitutive expression with the mRNA
390 having a Poisson-like distribution (Figure S10B); (iii) small k_{on} and large k_{off} , which leads to
391 most cells being silent (Figure S10C); (iv) and large k_{on} and large k_{off} , which leads to
392 constitutive expression (Figure S10D).

393 We generate simulated data for 100 cells from the four cases above and start with no
394 technical noise or cell size confounding. Within each case, we vary k_{on} , k_{off} , and s and use
395 relative absolute error $|\hat{\theta} - \theta|/\theta$ as a measurement of accuracy (Figure S11). Our results show
396 that genes with large k_{on} and small k_{off} (shown as the black curves in Figure S11) have the
397 largest estimation errors of the bursting parameters. Statistically it is hard to distinguish these
398 constitutively expressed genes from genes with large k_{on} and large k_{off} and thus the kinetic
399 parameters in this case cannot be accurately estimated, which has been previously reported [25,
400 45]. Furthermore, the estimation errors are large for genes with small k_{on} , large k_{off} , and small
401 s (shown as red curves in Figure S11) due to lack of cells with nonzero expression. The
402 standard errors and confidence intervals of the estimated kinetics from bootstrap resampling
403 further confirm the underperformance for the above two classes (Table S2). This emphasizes
404 the need to adopt the Bayes categorization framework as a first step so that kinetic parameters

405 are stably estimated only for genes whose both alleles are bursty. For genes whose alleles are
406 perpetually silent or constitutively expressed across cells, there is no good method, nor any
407 need, to estimate their bursting parameters.

408 Importantly, we see that the estimation bias in transcription rate s and deactivation rate
409 k_{off} cancel – over/under estimation of s is compensated by over/under estimation of k_{off} – and
410 as a consequence the burst size s/k_{off} can be more stably estimated than either parameter
411 alone, especially when $k_{on} \ll k_{off}$ (shown as red curves in Figure S11). This is further
412 confirmed by empirical results that allelic burst size has much higher correlation (0.746 from the
413 mouse blastocyst dataset and 0.692 from the human fibroblast dataset) than allelic transcription
414 and deactivation rate (0.464 and 0.265 for mouse blastocyst, and 0.458 and 0.33 for human
415 fibroblast) (Figure S12). For this reason, all of our results on real data are based on s/k_{off} and
416 we do not consider s and k_{off} separately.

417 We further carry out power analysis on the testing of differential burst frequency and
418 burst size between the two alleles. The null hypothesis is both alleles sharing the same bursting
419 kinetics ($k_{on}^A = k_{on}^B = 0.2, k_{off}^A = k_{off}^B = 0.2, s^A = s^B = 50$), while the alternative hypotheses with
420 differential burst frequency or burst size are shown in the legends in Figure S13. The detailed
421 setup of the simulation procedures are as follows. (i) Simulate the true allele-specific read
422 counts Y^A and Y^B across 100 cells from the Poisson-Beta model under the alternative
423 hypothesis. Technical noise is then added based on the noise model described earlier with
424 technical noise parameters $\{\alpha, \beta, \kappa, \tau\}$ estimated from the mouse blastocyst cell dataset. (ii)
425 Apply SCALE to the observed expression level Q^A and Q^B , which returns p -value for testing
426 differential burst size or burst frequency. If the p -value is less than the significance level, we
427 reject the null hypothesis. (iii) Repeat (i) and (ii) N times with the power estimated as
428 $\frac{\text{Number of } p\text{-values } \leq 0.05}{N}$. Our results indicate that the testing of burst frequency and burst size
429 have similar power overall with relatively reduced power if the difference in allelic burst size is
430 due to difference in the deactivation rate k_{off} .

431 We then simulate allele-specific counts from the full model including technical noise as
432 well as variations in cell size with the ground truth $k_{on}^A = k_{on}^B = k_{off}^A = k_{off}^B = 0.2, s^A = s^B =$
433 100 (bursty with small activation and deactivation rate). For parameters quantifying the degree
434 of technical noise, we use the estimates from the mouse blastocyst cells (Figure S5A) as well as
435 the human fibroblast cells (Figure S5B). Cell sizes are simulated from a normal distribution with
436 mean 0 and standard deviation 0.1 and 0.01. We run SCALE under four different settings: (i) in

437 its default setting, (ii) without accounting for cell size, (iii) without adjusting for technical
438 variability, (iv) not in an allele-specific fashion but using total coverage as input. Each is
439 repeated 5000 times with a sample size of 100 and 400 cells, respectively. Relative estimation
440 errors of burst size and burst frequency are summarized across all simulation runs. Our results
441 show that SCALE in its default setting has the smallest estimation errors for both burst size and
442 burst frequency (Figure S14-S15). Not surprisingly, cell size has larger effect on burst size
443 estimation than burst frequency estimation, while technical variability leads to biased estimation
444 of both burst frequency and burst size. The estimates taking total expression instead of ASE as
445 input are completely off. Furthermore, the estimation accuracy improved as the number of cells
446 increased. These results indicate the necessity to profile transcriptional kinetics in an allele-
447 specific fashion with adjustment of technical variability and cell size.

448 **Discussion**

449 We propose SCALE, a statistical framework to study ASE using scRNA-seq data. The input
450 data to SCALE are allele-specific read counts at heterozygous loci across all cells. In the two
451 datasets that we analyzed, we use the F1 mouse crossing and the bulk-tissue sequencing to
452 profile the true heterozygous loci. When these are not available, scRNA-seq itself can be used
453 to retrieve allele-specific expression and more specifically haplotype, as illustrated in Edsgard et
454 al. [46]. SCALE estimates parameters that characterize allele-specific transcriptional bursting,
455 after accounting for technical biases in scRNA-seq and size differences between cells. This
456 allows us to detect genes that exhibit allelic differences in burst frequency and burst size, and
457 genes whose alleles show coordinated or repulsed bursting patterns. Differences in mean
458 expression between the two alleles have long been observed in bulk RNA-seq. By scRNA-seq,
459 we now move beyond the mean and characterize the difference in expression distributions
460 between the two alleles, specifically in terms of their transcriptional bursting parameters.

461 Transcriptional bursting is a fundamental property of gene expression, yet its global
462 patterns in the genome has not been well characterized, and most studies consider bursting at
463 the gene level by ignoring the allelic origin of transcription. In this paper, we reanalyzed the
464 Deng et al. [2] and Borel et al. [17] data. We confirmed the findings from Levesque and Raj [32]
465 and Deng et al. [2] that for most genes across the genome there is no sufficient evidence
466 against the assumption of independent bursting with shared bursting kinetics between the two
467 alleles. For genes where significant deviations are observed, SCALE allows us to attribute the
468 deviation to differential bursting kinetics and/or non-independent bursting between the two
469 alleles.

470 More specifically, for genes that are transcribed in a “bursty” fashion, we compared the
471 burst frequency and burst size, between their two alleles. For both scRNA-seq datasets, we
472 identify significant number of genes whose allele-specific burstings differ in the burst frequency
473 but not in the burst size. Our findings provide evidence that burst frequency, which represents
474 the rate of gene activation, is modified in *cis*, and that burst size, which represents the ratio of
475 transcription rate to gene inactivation rate, is less likely to be modulated in *cis*. Although our
476 testing framework may have slightly reduced power in detecting differential deactivation rate
477 (Figure S13), the regulation in burst size can either result from a global *trans* factor or extrinsic
478 factors that acts upon both alleles. Similar findings have been previously reported, from different
479 perspectives and on different scales, using various technologies, platforms, and model
480 organisms [31, 36, 41-43].

481 It is worth noting that the estimated bursting parameters by SCALE are normalized by
482 the decay rate, where the inverse $1/d$ denotes the average life time of an mRNA molecule.
483 Here we implicitly make the assumptions that for each allele, the gene-specific decay rates (d_g^A
484 and d_g^B) are constant, and thus the estimated allelic burst frequencies are the ratio of true burst
485 frequency over decay rate (that is $k_{on,g}^A/d_g^A$ and $k_{on,g}^B/d_g^B$). The decay rates, however, cancel
486 out in the numerator and denominator in the allelic burst sizes, $s_g^A/k_{off,g}^A$ and $s_g^B/k_{off,g}^B$.
487 Therefore, the differences that we observe in the allelic burst frequencies can also potentially be
488 due to differential decay rates between the two alleles, which has been previously reported to
489 be regulated by microRNAs [47].

490 It is also important to note that 44% of the genes found to be significant for differential
491 burst frequency are not significant in the allelic imbalance test based on mean expression
492 across cells. This suggests that expression quantitative trait loci (eQTL) affecting gene
493 expression through modulation of bursting kinetics is likely to escape detection in existing eQTL
494 studies by bulk sequencing, especially when burst size and burst frequency change in different
495 directions. This is further underscored by the study of Wills et al. [48], which measured the
496 expression of 92 genes affected by Wnt signaling in 1,440 single cells from 15 individuals, and
497 then correlated SNPs with various gene-expression phenotypes. They found bursting kinetics as
498 characterized by burst size and burst frequency to be heritable, thus suggesting the existence of
499 bursting-QTLs. Taken together, these results should further motivate more large scale genome-
500 wide studies to systematically characterize the impact of eQTLs on various aspects of
501 transcriptional bursting.

502 Kim et al. [31] described a statistical framework to quantify the extent of stochastic ASE
503 in scRNA-seq data by using of spike-ins, where stochastic ASE is defined as excessive
504 variability in the ratio of the expression level of the paternal (or maternal) allele between cells
505 after controlling for mean allelic expression levels. While they attributed 18% of the stochastic
506 ASE to biological variability, they did not examine what biological factors lead to these
507 stochastic ASE. In this paper, we attribute the observed stochastic ASE to difference in allelic
508 bursting kinetics. By studying bursting kinetics in an allele-specific manner, we can compare the
509 transcriptional differences between the two alleles at a finer scale.

510 Kim and Marioni [25] described a procedure to estimate bursting kinetic parameters
511 using scRNA-seq data. Our method differs from Kim and Marioni [25] in several ways. First, our
512 model is an allele-specific model that infers kinetic parameters for each allele separately, thus
513 allowing comparisons between alleles. Second, we infer kinetic parameters based on the
514 distribution of “true expression” rather than the distribution of observed expression. We are able
515 to do this through the use of a simple and novel deconvolution approach, which allows us to
516 eliminate the impact of technical noise when making inference on the kinetic parameters.
517 Appropriate modeling of technical noise, in particular, gene dropouts, is critical in this context,
518 as failing to do so could lead to the overestimation of k_{off} . Third, we employ a gene
519 categorization procedure prior to fitting the bursting model. This is important because the
520 bursting parameters can only be reliably estimated for genes that have sufficient expression and
521 that are bursty.

522 As a by-product, SCALE also allows us to rigorously test, for scRNA-seq data, whether
523 the paternal and maternal alleles of a gene are independently expressed. In both scRNA-seq
524 datasets we analyzed, we identified more genes whose allele-specific burstings are in a
525 coordinated fashion than those in a repulsed fashion. The tendency towards coordination is not
526 surprising, since the two alleles of a gene share the same nuclear environment and thus the
527 same ensemble of transcription factors. We are aware that this degree of coordination can also
528 arise from the mixture of non-homogeneous cell populations, e.g., different lineages of cells
529 during mouse embryonic development, as we combine the early-, mid-, and late-blastocyst cells
530 to gain a large enough sample size. While it is possible that this might lead to false positives in
531 identifying coordinated bursting events, it will result in a decrease in power for the testing of
532 differential bursting kinetics. Given the amount of stochasticity that is observed in the allele-
533 specific expression data, how to define cell sub-types and how to quantify between-cell
534 heterogeneity need further investigation.

535 **Conclusions**

536 We have developed SCALE, a statistical framework for systematic characterization of ASE
537 using data generated from scRNA-seq experiments. Our approach allows us to profile allele-
538 specific bursting kinetics while accounting for technical variability and cell size difference. For
539 genes that are classified as biallelic bursty through a Bayes categorization framework, we
540 further examine whether transcription of the paternal and maternal alleles are independent, and
541 whether there are any kinetic differences, as represented by bursty frequency and burst size,
542 between the two alleles. Our results on the re-analysis of Deng et al. [2] and Borel et al. [17]
543 provide insights into the extent of differences, coordination, and repulsion between alleles in
544 transcriptional bursting.

545 **Methods**

546 **Input for endogenous RNAs and exogenous spike-ins**

547 For endogenous RNAs, SCALE takes as input the observed allele-specific read counts at
548 heterozygous locus Q_{cg}^A and Q_{cg}^B , with adjustment by library size factor:

$$549 \quad \eta_c = \text{median}_g \frac{Q_{cg}^A + Q_{cg}^B}{[\prod_{c^*=1}^C (Q_{c^*g}^A + Q_{c^*g}^B)]^{1/C}}.$$

550 In addition, for spike-ins, SCALE takes as input the true concentrations of the spike-in
551 molecules, the lengths of the molecules, as well as the depths of coverage for each spike-in
552 sequence across all cells (Table S1A-S1C). The true concentration of each spike-in molecule is
553 calculated according to the known concentration (denoted as C attomoles/uL) and the dilution
554 factor (x40000):

$$555 \quad \frac{C \times 10^{-18} \text{ moles/uL} \times 6.02214 \times 10^{23} \text{ mole}^{-1} \text{ (Avogadro constant)}}{40000 \text{ (dilution factor)}}.$$

556 The observed number of reads for each spike-in is calculated by adjusting for the library size
557 factor, the read length, and the length of the spike-in RNA. The bioinformatic pipeline to
558 generate the input for SCALE is included in Supplementary Methods.

559 **Empirical Bayes method for gene categorization**

560 We propose an empirical Bayes method that categorizes gene expressions across cells into
561 silent, monoallelic, biallelic states based on their ASE data. Without loss of generality, we focus
562 on one gene here with the goal of determining the most likely gene category based on its ASE
563 pattern. Let n_c^A and n_c^B be the allele-specific read counts in cell c for allele A and B, respectively.
564 For *each* cell, there are four different categories based on its ASE – $\{\emptyset, A, B, AB\}$ corresponding

565 to scenarios where both alleles are off, only A allele is expressed, only B allele is expressed,
 566 and both alleles are expressed, respectively. Let $k \in \{1,2,3,4\}$ represent this cell-specific
 567 category. The log-likelihood for the gene across all cells can be written as:

$$568 \quad \log(\mathcal{L}(\theta|n^A, n^B)) = \log \prod_c f(n_c^A, n_c^B | \theta) = \sum_c \log \left[\sum_{k=1}^4 \varphi_k f_k(n_c^A, n_c^B | \epsilon, a, b) \right],$$

569 where the parameters are $\theta = \{\varphi_1, \dots, \varphi_4, \epsilon, a, b\}$ with $\sum_{k=1}^4 \varphi_k = 1$ and each f_k is a density
 570 function parameterized by ϵ, a, b . ϵ is the per-base sequencing error rate, and a and b are
 571 hyper-parameters for a Beta distribution, where $\theta_c \sim \text{Beta}(a, b)$ corresponds to the relative
 572 expression of A allele when both alleles are expressed. It is easy to show that

$$573 \quad f_1(n_c^A, n_c^B | \epsilon, a, b) \propto \epsilon^{n_c^A + n_c^B},$$

$$574 \quad f_2(n_c^A, n_c^B | \epsilon, a, b) \propto (1 - \epsilon)^{n_c^A} \epsilon^{n_c^B},$$

$$575 \quad f_3(n_c^A, n_c^B | \epsilon, a, b) \propto \epsilon^{n_c^A} (1 - \epsilon)^{n_c^B},$$

$$576 \quad f_4(n_c^A, n_c^B | \epsilon, a, b) \propto \int_0^1 [\theta_c(1 - \epsilon) + (1 - \theta_c)\epsilon]^{n_c^A} [\theta_c\epsilon + (1 - \theta_c)(1 - \epsilon)]^{n_c^B} \frac{\theta_c^{a-1} (1 - \theta_c)^{b-1}}{B(a, b)} d\theta_c.$$

577 ϵ can be estimated using sex chromosome mismatching or be prefixed at the default value,
 578 0.001. We require $a = b \geq 3$ in the prior on θ_c so that the AB state is distinguishable from the A
 579 and B states. This is a reasonable assumption in that most genes have balanced ASE on
 580 average and the use of Beta distribution allows variability of allelic ratio across cells. We adopt
 581 an EM algorithm for estimation, with Z being the missing variables:

$$582 \quad Z_{ck} = \begin{cases} 1 & \text{if cell } c \text{ belongs to category } k \\ 0 & \text{otherwise} \end{cases}.$$

583 The complete-data log-likelihood is given as

$$584 \quad \log(\mathcal{L}(\theta|n^A, n^B, Z)) = \log \left[\sum_c \prod_{k=1}^4 f_k(n_c^A, n_c^B | \epsilon, a, b)^{Z_{ck}} \varphi_k^{Z_{ck}} \right]$$

$$585 \quad = \sum_c \sum_{k=1}^4 Z_{ck} \log(\varphi_k) + \sum_c \sum_{k=1}^4 Z_{ck} \log[f_k(n_c^A, n_c^B | \epsilon, a, b)].$$

586 For each cell, we assign the state that has the maximum posterior probability and only keep a
 587 cell if its maximum posterior probability is greater than 0.8. Let N_\emptyset, N_A, N_B , and N_{AB} be the
 588 number of cells in state $\{\emptyset\}, \{A\}, \{B\}$, and $\{AB\}$, respectively. We then assign a gene to be: (i)
 589 silent if $N_A = N_B = N_{AB} = 0$; (ii) A-allele monoallelic if $N_A > 0, N_B = N_{AB} = 0$; (iii) B-allele
 590 monoallelic if $N_B > 0, N_A = N_{AB} = 0$; (iv) biallelic otherwise (biallelic bursty if $0.05 \leq$
 591 $(N_A + N_{AB}) / (N_\emptyset + N_A + N_B + N_{AB}) \leq 0.95$ and $0.05 \leq (N_B + N_{AB}) / (N_\emptyset + N_A + N_B + N_{AB}) \leq 0.95$).

592 Parameter estimation for Poisson-Beta hierarchical model

593 Since exogenous spike-ins are added in a fixed amount and don't undergo transcriptional
 594 bursting, they can be used to directly estimate the technical-variability-associated parameters
 595 $\{\alpha, \beta, \kappa, \tau\}$ that are shared across all cells from the same sequencing batch. Specifically, we use
 596 non-zero read counts to estimate α and β through log-linear regression:

$$597 \quad Q_{cg} \sim \text{Poisson}\left(\alpha(Y_{cg})^\beta\right),$$

598 where $Q_{cg} > 0$, capture and sequencing efficiencies are confounded in α and amplification bias
 599 is modeled by β (Figure S5). We then use the Nelder-Mead simplex algorithm to jointly optimize
 600 κ and τ , which models the probability of non-dropout, using the likelihood function:

$$601 \quad \log\left(\mathcal{L}(\kappa, \tau | Q, Y, \hat{\alpha}, \hat{\beta})\right) = \prod_c \prod_g \log\left\{\text{pPoisson}\left(Q_{cg}, \hat{\alpha}(Y_{cg})^{\hat{\beta}}\right) \text{expit}(\kappa + \tau \log Y_{cg}) + \right. \\
 602 \quad \left. (1 - \text{expit}(\kappa + \tau \log Y_{cg})) \mathbb{1}(Q_{cg} = 0)\right\},$$

603 where $\text{pPoisson}(x, y)$ specifies the Poisson likelihood of getting x from a Poisson distribution
 604 with mean y . This log-likelihood function together with the estimated parameters decomposes
 605 the zero read counts ($Q_{cg} = 0$) into being from the dropout events or from being sampled as
 606 zero from the Poisson sampling during sequencing (Figure S5A).

607 The allele-specific kinetic parameters are estimated via the moment estimator methods,
 608 which is more computational efficient than the Gibbs sampler method adopted by Kim and
 609 Marioni [25]. For each gene, the distribution moments of the A allele given true expression
 610 levels Y_c^A and Y_c^B are:

$$611 \quad m_1^A \equiv \frac{E[\sum_c Y_c^A]}{\sum_c \phi_c} = \frac{k_{on}^A s^A}{k_{on}^A + k_{off}^A}$$

$$612 \quad m_2^A \equiv \frac{E[\sum_c Y_c^A (Y_c^A - 1)]}{\sum_c \phi_c^2} = \frac{k_{on}^A (k_{on}^A + 1) (s^A)^2}{(k_{on}^A + k_{off}^A) (k_{on}^A + k_{off}^A + 1)}$$

$$613 \quad m_3^A \equiv \frac{E[\sum_c Y_c^A (Y_c^A - 1) (Y_c^A - 2)]}{\sum_c \phi_c^3} = \frac{k_{on}^A (k_{on}^A + 1) (k_{on}^A + 2) (s^A)^3}{(k_{on}^A + k_{off}^A) (k_{on}^A + k_{off}^A + 1) (k_{on}^A + k_{off}^A + 2)}.$$

614 Solving this system of three equations, we have:

$$615 \quad \hat{k}_{on}^A = \frac{-2\left(-m_1^A (m_2^A)^2 + (m_1^A)^2 m_3^A\right)}{-m_1^A (m_2^A)^2 + 2(m_1^A)^2 m_3^A - m_2^A m_3^A}$$

$$616 \quad \hat{k}_{off}^A = \frac{2\left((m_1^A)^2 - m_2^A\right) (m_1^A m_2^A - m_3^A) \left(m_1^A m_3^A - (m_2^A)^2\right)}{\left((m_1^A)^2 m_2^A - 2(m_2^A)^2 + m_1^A m_3^A\right) \left(2(m_1^A)^2 m_3^A - m_1^A (m_2^A)^2 - m_2^A m_3^A\right)}$$

$$617 \quad \hat{s}^A = \frac{-m_1^A (m_2^A)^2 + 2(m_1^A)^2 m_3^A - m_2^A m_3^A}{(m_1^A)^2 m_2^A - 2(m_2^A)^2 + m_1^A m_3^A}.$$

618 Substituting A with B we get the kinetic parameters for the B allele. To get the sample moments,
 619 we propose a novel histogram repiling method that gives the sample distribution and sample
 620 moment estimates of the true expression from the distribution of the observed expression
 621 (Figure S7). Specifically, for each gene we denote $c(Q)$ as the number of cells with observed
 622 expression Q and $n(Y)$ as the number of cells with the corresponding true expression Y . $c(Q)$
 623 follows a Binomial distribution indexed at $n(Y)$ with probability of no dropout:

$$624 \quad c(Q) \sim \text{Binomial}(n(Y), \text{expit}(\hat{\kappa} + \hat{\tau} \log Y)).$$

625 Then,

$$626 \quad \hat{n}(Y) = \frac{c(Q)}{\text{expit}(\hat{\kappa} + \hat{\tau} \log Y)} = \frac{c(Q)}{\text{expit}\left(\hat{\kappa} + \frac{\hat{\tau}}{\hat{\beta}} \log \frac{Q}{\hat{\alpha}}\right)}.$$

627 These moment estimates of the kinetic parameters are sometimes negative as is pointed out by
 628 Kim and Marioni [25]. By *in silico* simulation studies, we investigate the estimation accuracy and
 629 robustness under different settings.

630 Hypothesis testing framework

631 We carry out a nonparametric bootstrap hypothesis testing procedure with the null hypothesis
 632 that the two alleles of a gene share the same kinetic parameters (Figure 4A-4B). The
 633 procedures are as follow.

634 (i) For gene g , let $\{Q_{1g}^A, Q_{2g}^A, \dots, Q_{ng}^A\}$ and $\{Q_{1g}^B, Q_{2g}^B, \dots, Q_{ng}^B\}$ be the observed allele-specific read
 635 counts. Estimate allele-specific kinetic parameters with adjustment of technical variability:

$$636 \quad \hat{\theta}^A = \{\hat{k}_{on,g}^A, \hat{k}_{off,g}^A, \hat{s}_g^A\}; \quad \hat{\theta}^B = \{\hat{k}_{on,g}^B, \hat{k}_{off,g}^B, \hat{s}_g^B\}.$$

637 (ii) Combine the $2n$ observed allelic measurements and draw samples of size $2n$ from the
 638 combined pool with replacement. Assign the first n with their corresponding cell sizes to
 639 allele A as $\{Q_{1g}^{A*}, Q_{2g}^{A*}, \dots, Q_{ng}^{A*}\}$, the next n to allele B $\{Q_{1g}^{B*}, Q_{2g}^{B*}, \dots, Q_{ng}^{B*}\}$. Estimate kinetic
 640 parameters with adjustment of technical variability from the bootstrap samples:

$$642 \quad \theta^{A*} = \{k_{on,g}^{A*}, k_{off,g}^{A*}, s_g^{A*}\}; \quad \theta^{B*} = \{k_{on,g}^{B*}, k_{off,g}^{B*}, s_g^{B*}\}.$$

641 Iterate this N times.

643 (iii) Compute the p -values:

$$644 \quad p = \frac{\sum \mathbb{1}(|\theta^{A*} - \theta^{B*}| \geq |\hat{\theta}^A - \hat{\theta}^B|)}{N}.$$

645 We adopt a Binomial test of allelic imbalance with the null hypothesis that the allelic ratio of the
 646 mean expression across all cells is 0.5. Chi-square test of independence is further performed to
 647 test whether the two alleles of a gene fire independently (Figure 4C). The observed number of

648 cells is from the direct output of the Bayes gene categorization framework. For all hypothesis
649 testing, we adopt FDR to adjust for multiple comparisons.

650 **Abbreviations**

651 scRNA-seq: single-cell RNA sequencing, ASE: allele-specific expression, SNP: single-
652 nucleotide polymorphism, RNA-seq: RNA sequencing, ME: monoallelic expression, RME:
653 random monoallelic expression, FISH: fluorescence *in situ* hybridization, EM: expectation-
654 maximization, FDR: false discovery rate, RPKM: reads per kilo base per million reads, PCA:
655 principal component analysis, QC: quality control, QTL: quantitative trait loci.

656 **Declarations**

657 We thank Dr. Daniel Ramsköld for providing dataset of the mouse preimplantation embryos, Dr.
658 Christelle Borel for providing dataset of the human fibroblast, and Cheng Jia, Dr. Arjun Raj, and
659 Dr. Uschi Symmons for helpful comments and suggestions. This work was supported by
660 National Institutes of Health (NIH) grant R01HG006137 to NRZ, and R01GM108600 and
661 R01HL113147 to ML. The authors declare that they have no competing interests.

662 **References**

- 663 1. Buckland PR: **Allele-specific gene expression differences in humans.** *Hum Mol Genet* 2004, **13**
664 **Spec No 2:**R255-260.
- 665 2. Deng Q, Ramsköld D, Reinius B, Sandberg R: **Single-cell RNA-seq reveals dynamic, random**
666 **monoallelic gene expression in mammalian cells.** *Science* 2014, **343:**193-196.
- 667 3. Gendrel AV, Attia M, Chen CJ, Diabangouaya P, Servant N, Barillot E, Heard E: **Developmental**
668 **dynamics and disease potential of random monoallelic gene expression.** *Dev Cell* 2014, **28:**366-
669 380.
- 670 4. Eckersley-Maslin MA, Spector DL: **Random monoallelic expression: regulating gene expression**
671 **one allele at a time.** *Trends Genet* 2014, **30:**237-244.
- 672 5. Eckersley-Maslin MA, Thybert D, Bergmann JH, Marioni JC, Flicek P, Spector DL: **Random**
673 **monoallelic gene expression increases upon embryonic stem cell differentiation.** *Dev Cell* 2014,
674 **28:**351-365.
- 675 6. Reinius B, Sandberg R: **Random monoallelic expression of autosomal genes: stochastic**
676 **transcription and allele-level regulation.** *Nat Rev Genet* 2015, **16:**653-664.
- 677 7. Reinius B, Mold JE, Ramsköld D, Deng Q, Johnsson P, Michaelsson J, Frisen J, Sandberg R:
678 **Analysis of allelic expression patterns in clonal somatic cells by single-cell RNA-seq.** *Nat Genet*
679 2016, **48:**1430-1435.
- 680 8. Björnsson HT, Albert TJ, Ladd-Acosta CM, Green RD, Rongione MA, Middle CM, Irizarry RA,
681 Broman KW, Feinberg AP: **SNP-specific array-based allele-specific expression analysis.** *Genome*
682 *Res* 2008, **18:**771-779.
- 683 9. Skelly DA, Johansson M, Madeoy J, Wakefield J, Akey JM: **A powerful and flexible statistical**
684 **framework for testing hypotheses of allele-specific gene expression from RNA-seq data.**
685 *Genome Res* 2011, **21:**1728-1737.

- 686 10. Leon-Novelo LG, McIntyre LM, Fear JM, Graze RM: **A flexible Bayesian method for detecting**
687 **allelic imbalance in RNA-seq data.** *BMC Genomics* 2014, **15**:920.
- 688 11. Castel SE, Levy-Moonshine A, Mohammadi P, Banks E, Lappalainen T: **Tools and best practices**
689 **for data processing in allelic expression analysis.** *Genome Biol* 2015, **16**:195.
- 690 12. Knight JC: **Allele-specific gene expression uncovered.** *Trends Genet* 2004, **20**:113-116.
- 691 13. Bell CG, Beck S: **Advances in the identification and analysis of allele-specific expression.**
692 *Genome Med* 2009, **1**:56.
- 693 14. de la Chapelle A: **Genetic predisposition to human disease: allele-specific expression and low-**
694 **penetrance regulatory loci.** *Oncogene* 2009, **28**:3345-3348.
- 695 15. Stegle O, Teichmann SA, Marioni JC: **Computational and analytical challenges in single-cell**
696 **transcriptomics.** *Nat Rev Genet* 2015, **16**:133-145.
- 697 16. Kolodziejczyk AA, Kim JK, Svensson V, Marioni JC, Teichmann SA: **The technology and biology of**
698 **single-cell RNA sequencing.** *Mol Cell* 2015, **58**:610-620.
- 699 17. Borel C, Ferreira PG, Santoni F, Delaneau O, Fort A, Popadin KY, Garieri M, Falconnet E, Ribaux P,
700 Guipponi M, et al: **Biased allelic expression in human primary fibroblast single cells.** *Am J Hum*
701 *Genet* 2015, **96**:70-80.
- 702 18. Chubb JR, Trcek T, Shenoy SM, Singer RH: **Transcriptional pulsing of a developmental gene.** *Curr*
703 *Biol* 2006, **16**:1018-1025.
- 704 19. Raj A, van Oudenaarden A: **Nature, nurture, or chance: stochastic gene expression and its**
705 **consequences.** *Cell* 2008, **135**:216-226.
- 706 20. Chong S, Chen C, Ge H, Xie XS: **Mechanism of transcriptional bursting in bacteria.** *Cell* 2014,
707 **158**:314-326.
- 708 21. Blake WJ, Balazsi G, Kohanski MA, Isaacs FJ, Murphy KF, Kuang Y, Cantor CR, Walt DR, Collins JJ:
709 **Phenotypic consequences of promoter-mediated transcriptional noise.** *Mol Cell* 2006, **24**:853-
710 865.
- 711 22. Fukaya T, Lim B, Levine M: **Enhancer Control of Transcriptional Bursting.** *Cell* 2016, **166**:358-368.
- 712 23. Raj A, Peskin CS, Tranchina D, Vargas DY, Tyagi S: **Stochastic mRNA synthesis in mammalian**
713 **cells.** *PLoS Biol* 2006, **4**:e309.
- 714 24. Suter DM, Molina N, Gatfield D, Schneider K, Schibler U, Naef F: **Mammalian genes are**
715 **transcribed with widely different bursting kinetics.** *Science* 2011, **332**:472-474.
- 716 25. Kim JK, Marioni JC: **Inferring the kinetics of stochastic gene expression from single-cell RNA-**
717 **sequencing data.** *Genome Biol* 2013, **14**:R7.
- 718 26. Brennecke P, Anders S, Kim JK, Kolodziejczyk AA, Zhang X, Proserpio V, Baying B, Benes V,
719 Teichmann SA, Marioni JC, Heisler MG: **Accounting for technical noise in single-cell RNA-seq**
720 **experiments.** *Nat Methods* 2013, **10**:1093-1095.
- 721 27. Pierson E, Yau C: **ZIFA: Dimensionality reduction for zero-inflated single-cell gene expression**
722 **analysis.** *Genome Biol* 2015, **16**:241.
- 723 28. Vallejos CA, Marioni JC, Richardson S: **BASiCS: Bayesian Analysis of Single-Cell Sequencing Data.**
724 *PLoS Comput Biol* 2015, **11**:e1004333.
- 725 29. Ding B, Zheng L, Zhu Y, Li N, Jia H, Ai R, Wildberg A, Wang W: **Normalization and noise reduction**
726 **for single cell RNA-seq experiments.** *Bioinformatics* 2015, **31**:2225-2227.
- 727 30. Qiu X, Hill A, Packer J, Lin D, Ma YA, Trapnell C: **Single-cell mRNA quantification and differential**
728 **analysis with Census.** *Nat Methods* 2017.
- 729 31. Kim JK, Kolodziejczyk AA, Illicic T, Teichmann SA, Marioni JC: **Characterizing noise structure in**
730 **single-cell RNA-seq distinguishes genuine from technical stochastic allelic expression.** *Nat*
731 *Commun* 2015, **6**:8687.
- 732 32. Levesque MJ, Raj A: **Single-chromosome transcriptional profiling reveals chromosomal gene**
733 **expression regulation.** *Nat Methods* 2013, **10**:246-248.

- 734 33. Kepler TB, Elston TC: **Stochasticity in transcriptional regulation: origins, consequences, and**
735 **mathematical representations.** *Biophys J* 2001, **81**:3116-3136.
- 736 34. Bix M, Locksley RM: **Independent and epigenetic regulation of the interleukin-4 alleles in CD4+**
737 **T cells.** *Science* 1998, **281**:1352-1354.
- 738 35. Levesque MJ, Ginart P, Wei Y, Raj A: **Visualizing SNVs to quantify allele-specific expression in**
739 **single cells.** *Nat Methods* 2013, **10**:865-867.
- 740 36. Padovan-Merhar O, Nair GP, Biaisch AG, Mayer A, Scarfone S, Foley SW, Wu AR, Churchman LS,
741 Singh A, Raj A: **Single mammalian cells compensate for differences in cellular volume and DNA**
742 **copy number through independent global transcriptional mechanisms.** *Mol Cell* 2015, **58**:339-
743 352.
- 744 37. Ramskold D, Luo S, Wang YC, Li R, Deng Q, Faridani OR, Daniels GA, Khrebtkova I, Loring JF,
745 Laurent LC, et al: **Full-length mRNA-Seq from single-cell levels of RNA and individual circulating**
746 **tumor cells.** *Nat Biotechnol* 2012, **30**:777-782.
- 747 38. Dadiani M, van Dijk D, Segal B, Field Y, Ben-Artzi G, Raveh-Sadka T, Levo M, Kaplow I,
748 Weinberger A, Segal E: **Two DNA-encoded strategies for increasing expression with opposing**
749 **effects on promoter dynamics and transcriptional noise.** *Genome Res* 2013, **23**:966-976.
- 750 39. Bartman CR, Hsu SC, Hsiung CC, Raj A, Blobel GA: **Enhancer Regulation of Transcriptional**
751 **Bursting Parameters Revealed by Forced Chromatin Looping.** *Mol Cell* 2016, **62**:237-247.
- 752 40. Sepulveda LA, Xu H, Zhang J, Wang M, Golding I: **Measurement of gene regulation in individual**
753 **cells reveals rapid switching between promoter states.** *Science* 2016, **351**:1218-1222.
- 754 41. Skinner SO, Xu H, Nagarkar-Jaiswal S, Freire PR, Zwaka TP, Golding I: **Single-cell analysis of**
755 **transcription kinetics across the cell cycle.** *Elife* 2016, **5**.
- 756 42. Ochiai H, Sugawara T, Sakuma T, Yamamoto T: **Stochastic promoter activation affects Nanog**
757 **expression variability in mouse embryonic stem cells.** *Sci Rep* 2014, **4**:7125.
- 758 43. Xu H, Sepulveda LA, Figard L, Sokac AM, Golding I: **Combining protein and mRNA quantification**
759 **to decipher transcriptional regulation.** *Nat Methods* 2015, **12**:739-742.
- 760 44. Li H, Handsaker B, Wysoker A, Fennell T, Ruan J, Homer N, Marth G, Abecasis G, Durbin R,
761 Genome Project Data Processing S: **The Sequence Alignment/Map format and SAMtools.**
762 *Bioinformatics* 2009, **25**:2078-2079.
- 763 45. Munsky B, Neuert G, van Oudenaarden A: **Using gene expression noise to understand gene**
764 **regulation.** *Science* 2012, **336**:183-187.
- 765 46. Edsgard D, Reinius B, Sandberg R: **scphaser: haplotype inference using single-cell RNA-seq data.**
766 *Bioinformatics* 2016, **32**:3038-3040.
- 767 47. Valencia-Sanchez MA, Liu J, Hannon GJ, Parker R: **Control of translation and mRNA degradation**
768 **by miRNAs and siRNAs.** *Genes Dev* 2006, **20**:515-524.
- 769 48. Wills QF, Livak KJ, Tipping AJ, Enver T, Goldson AJ, Sexton DW, Holmes C: **Single-cell gene**
770 **expression analysis reveals genetic associations masked in whole-tissue experiments.** *Nat*
771 *Biotechnol* 2013, **31**:748-752.

772

773 **Figure Legends**

774 **Figure 1. Allele-specific transcriptional bursting and gene categorization by**
775 **single-cell ASE.** (A) Transcription from DNA to RNA occurs in bursts, where genes
776 switch between the “ON” and the “OFF” states. k_{on} , k_{off} , s , and d are activation,
777 deactivation, transcription, and mRNA decay rate in the kinetic model respectively. (B)

778 Transcriptional bursting of the two alleles of a gene give rise to cells expressing neither,
779 one, or both alleles of a gene, sampled as vertical snapshots along the time axis.
780 Partially adapted from Reinius and Sandberg [6]. (C) Empirical Bayes framework that
781 categorizes each gene as silent, monoallelic and biallelic (biallelic bursty, one-allele
782 constitutive, and both-alleles constitutive) based on ASE data with single-cell resolution.

783 **Figure 2. Overview of analysis pipeline of SCALE.** SCALE takes as input allele-
784 specific read counts at heterozygous loci and carries out three major steps: (i) an
785 empirical Bayes method for gene classification, (ii) a Poisson-Beta hierarchical model to
786 estimate allele-specific transcriptional kinetics with adjustment of technical variability
787 and cell size, (iii) a hypothesis testing framework to test the two alleles of a gene have
788 differential bursting kinetics and/or non-independent firing.

789 **Figure 3. Allele-specific transcriptional kinetics of 7486 genes from 122 mouse**
790 **blastocyst cells.** (A) Burst frequency of the two alleles has a correlation of 0.852. 425
791 genes show significant allelic difference in burst frequency after FDR control. (B) Burst
792 size of the two alleles has a correlation of 0.746. Two genes show significant allelic
793 difference in burst size. X-chromosome genes as positive controls show significant
794 higher burst frequencies of the maternal alleles than those of the paternal alleles. The p -
795 values for allelic burst size difference (bottom right panels) are uniformly distributed as
796 expected under the null, whereas those for allelic burst frequency difference (bottom left
797 panels) have a spike below significance level after FDR control.

798 **Figure 4. Examples of significant genes from hypothesis testing.** (A) The two
799 alleles of the gene have significantly differential burst frequency from the bootstrap-
800 based testing. (B) The two alleles of the gene have significantly differential burst size
801 and burst frequency. (C) The two alleles of the gene fire non-independently from the
802 chi-square test of independence.

803 **Figure 5. Testing of bursting kinetics by scRNA-seq and testing mean difference**
804 **by bulk-tissue sequencing.** (A) Venn diagram of genes that are significant from testing
805 of shared burst frequency and allelic imbalance. *Also includes the two genes that are
806 significant from testing of shared burst size. Change in burst frequency and burst size in

807 the same direction leads to higher detection power of allelic imbalance; change in
808 different direction leads to allelic imbalance testing being underpowered. (B) Gene
809 *Dhrs7* whose two alleles have bursting kinetics in different direction and gene *Gprc5a*
810 whose two alleles have bursting kinetics in the same direction. *Dhrs7* is significant from
811 testing of differential allelic bursting kinetics; *Gprc5a* is significant from the testing of
812 mean difference between the two alleles.

813 **Figure 6. Allele-specific transcriptional kinetics of 2277 genes from 104 human**
814 **fibroblast cells.** (A) Burst frequency of the two alleles has a correlation of 0.859. 26
815 genes show significant allelic difference in burst frequency after FDR. (B) Burst size of
816 the two alleles has a correlation of 0.692. One gene has significant allelic difference in
817 burst size. The results are concordant with the findings from the mouse embryonic
818 development study.

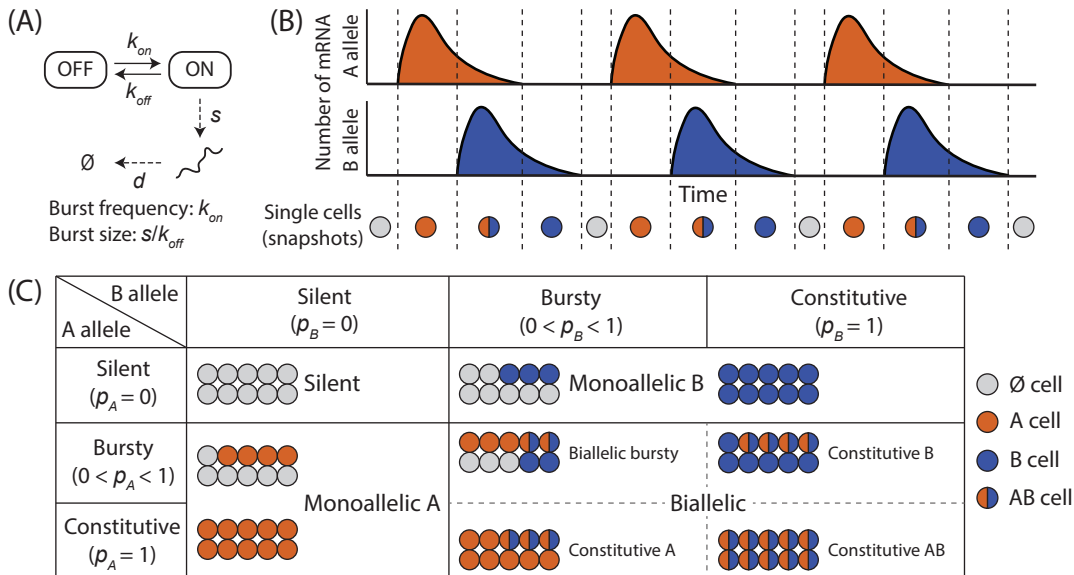


Figure 1

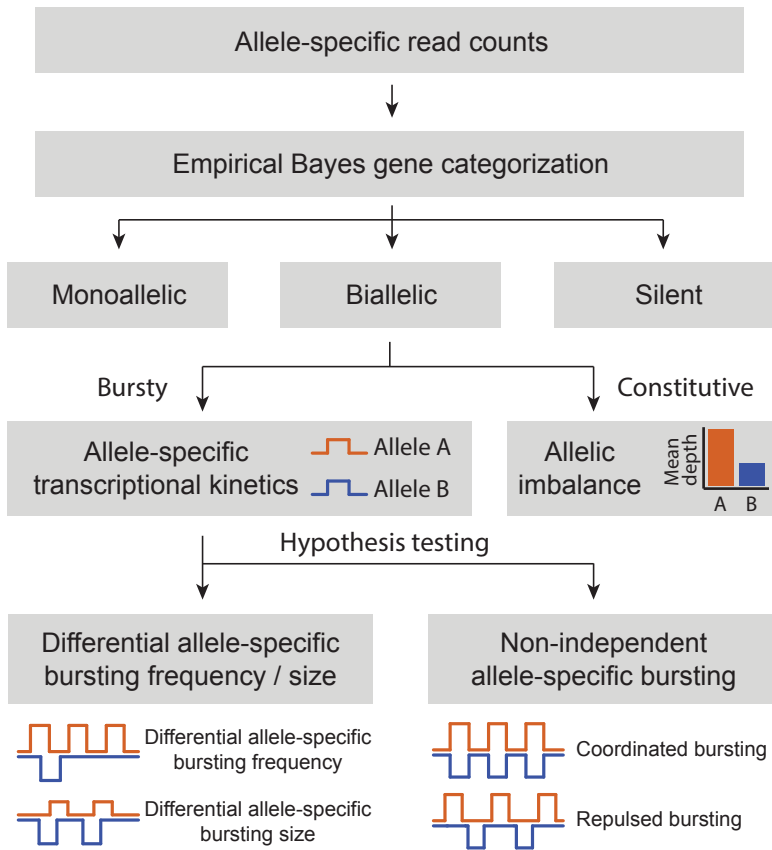
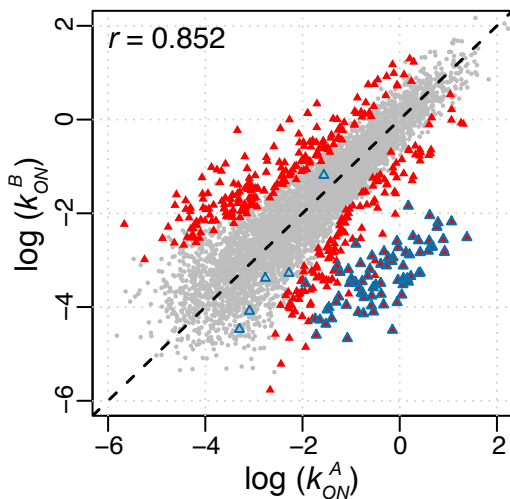
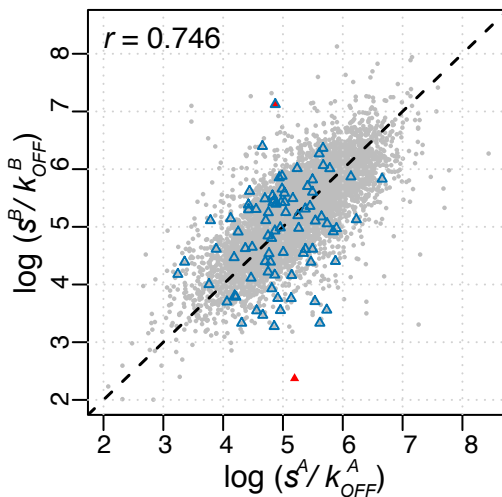


Figure 2

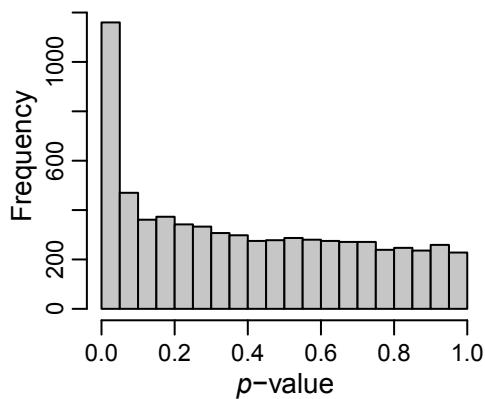
(A) Allele-specific burst frequency



(B) Allele-specific burst size



H0: $k_{onA} = k_{onB}$; Ha: $k_{onA} \neq k_{onB}$



H0: $sizeA = sizeB$; Ha: $sizeA \neq sizeB$

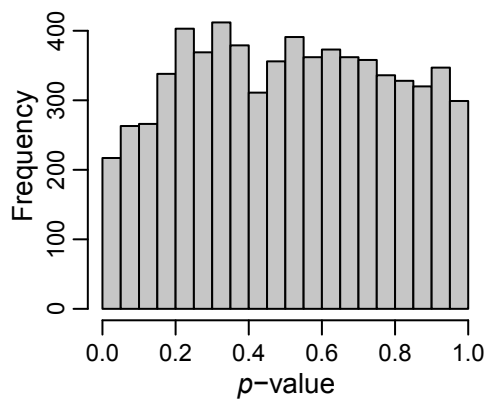
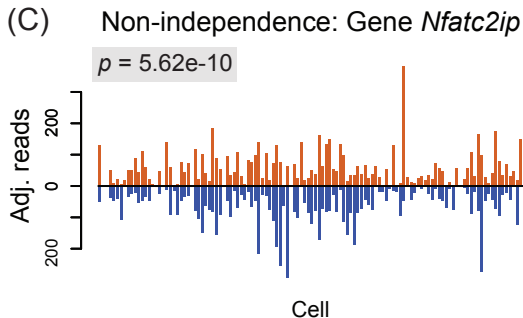
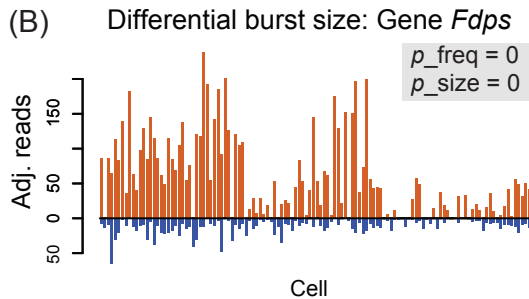
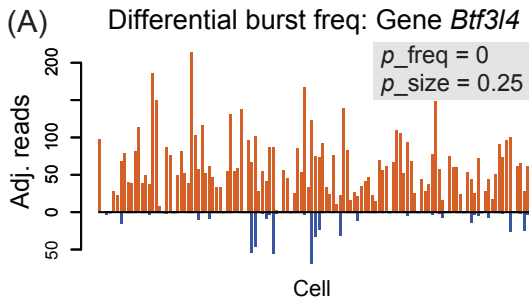


Figure 3



Observed (Bayes framework)

	A off	A on
B off	8	5
B on	5	101

Expected

	A off	A on
B off	1.4	11.6
B on	11.6	94.4

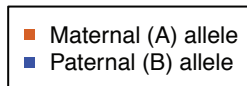


Figure 4

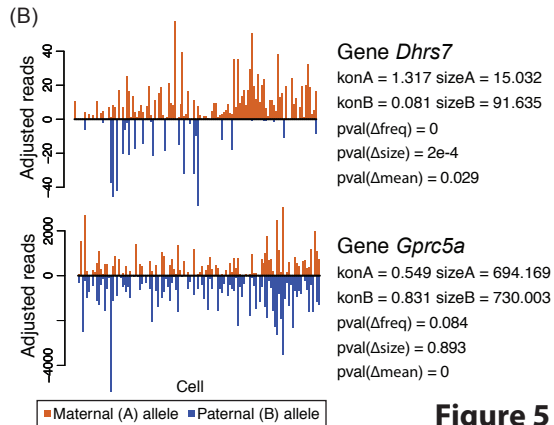
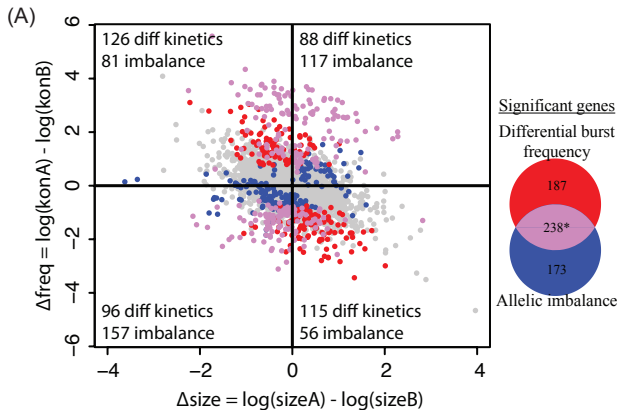
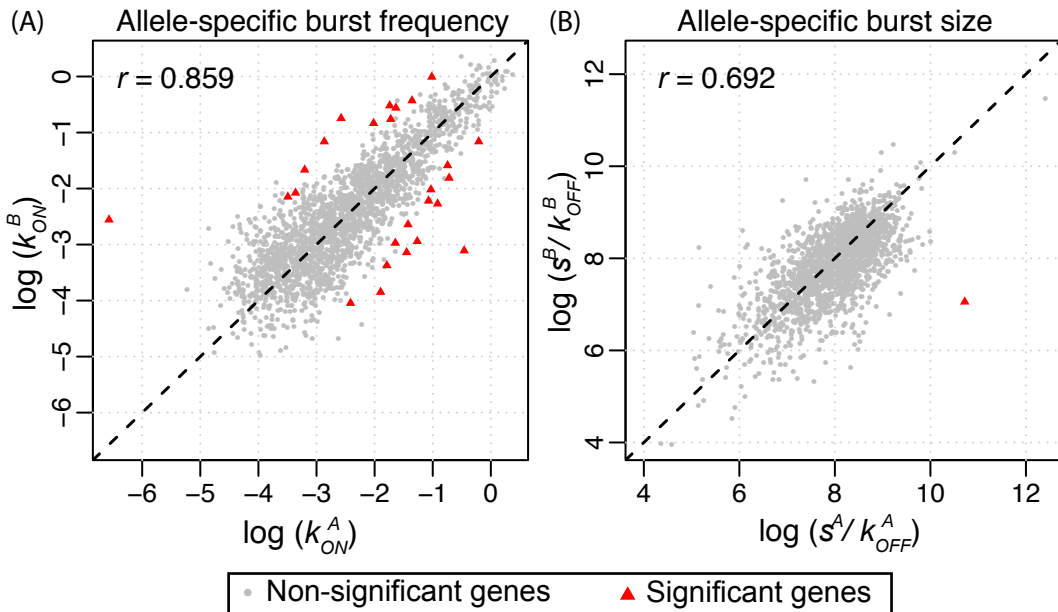
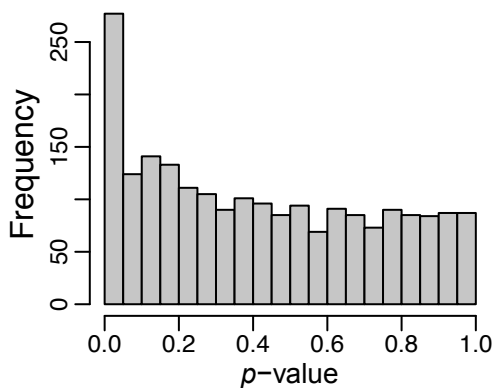


Figure 5



H0: $k_{ON}^A = k_{ON}^B$; Ha: $k_{ON}^A \neq k_{ON}^B$



H0: $size^A = size^B$; Ha: $size^A \neq size^B$

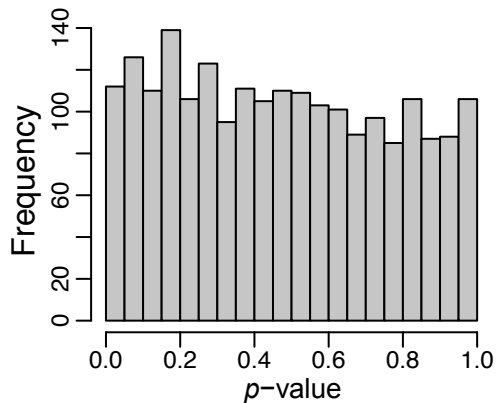


Figure 6